Microporous and Mesoporous Materials 147 (2012) 267–273

Contents lists available at ScienceDirect

Microporous and Mesoporous Materials

journal homepage: www.elsevier.com/locate/micromeso

Growth of *Escherichia coli* and *Salmonella typhi* inhibited by fractal silver nanoparticles supported on zeolites

Roberto Guerra [a], Enrique Lima [b,*], Margarita Viniegra [a], Ariel Guzmán [c], Víctor Lara [a]

[a] Universidad Autónoma Metropolitana, Iztapalapa, Av. San Rafael Atlixco No. 186, Col. Vicentina, CP 09340 México DF, Mexico
[b] Instituto de Investigaciones en Materiales, Universidad Nacional Autónoma de México, Circuito exterior s/n, Cd. Universitaria, Del. Coyoacán, CP 04510 México DF, Mexico
[c] Instituto Politécnico Nacional – ESIQIE, Av. IPN UPALM Edif. 7, Zacatenco 07738 México DF, Mexico

ARTICLE INFO

Article history:
Received 12 April 2011
Received in revised form 15 June 2011
Accepted 25 June 2011
Available online 2 July 2011

Keywords:
Zeolite
Escherichia coli
Salmonella
Silver particles
Porous

ABSTRACT

Silver nanoparticles were dispersed on clinoptilolite zeolite. These materials were evaluated as biocides for *Escherichia coli* and *Salmonella typhi*. Ag-zeolites were shown to be efficient in eliminating both *E. coli* and *S. typhi* present in nutritive media. Particularly, *E. coli* was eliminated at very short times. In the presence of a zeolite free of silver, bacteria use the zeolite to reproduce rapidly.

© 2011 Elsevier Inc. All rights reserved.

1. Introduction

The threat of water-borne infectious diseases is well known. Water is easily contaminated by bacteria. Some bacteria can be positively used for the degradation of some organic molecules [1,2]; often, unfortunately, they are unsuitable, and the increasing number of epidemics reveals that transmission of pathogens by drinking water is currently a significant problem. Thus, antimicrobial agents are required to inhibit the reproduction of pathogens. Numerous antimicrobial agents have been used. Their efficiencies are determined by several physicochemical factors [3–5]. Many of them, however, are toxic, which makes them undesirable for applications in sensitive media such as drinking water, foods or textiles. In this sense, silver is a non-toxic, non-tolerant disinfectant that can significantly reduce many bacterial infections [6]. The antimicrobial activity of silver species, particularly ions, is well documented. In fact, silver has been frequently used for wound management in the form of $AgNO_3$ solutions [7–9]. At present, silver remains an agent used in wound management because of limitations in the prescription of antibiotics in many cases [10]. It is expected that the high specific surface area and high fraction of surface atoms of silver nanoparticles will lead to high bactericide activity when compared to bulk silver metal [11,12]. Furthermore, when used in reasonable amounts, silver metal does not negatively affect the human body. In the catalysis field, in order to maximise the active surface, the catalysts are frequently composed of a metal (active phase) dispersed on an inorganic matrix (support) [13,14]. This approach could be used to prepare a supported silver phase that is able to inhibit the growth of pathogens. Supports, however, differ greatly regarding their physicochemical properties, which in turn drive the properties of the metal being supported [15–17]. Silver-supported particles can be used to inhibit the growth of pathogens, by either adding the particles directly to water or incorporating them in several materials, for example, clothes. With these applications in mind, our goal is to study the efficiency of silver supported on a clinoptilolite zeolite as a system to avoid bacterial growth. We have selected this support because it occurs naturally as a mineral and has easily tuneable physicochemical properties [18,19]. Further, zeolites have been previously tested for adsorption of other types of bacteria [20]. Here, zeolite-supported silver was tested as a bactericide for *Escherichia coli* and *Salmonella*.

2. Experimental procedure

2.1. Clinoptilolite source

A clinoptilolite-rich tuff from Etla, Oaxaca in southeast Mexico was ground and sieved (0.15 mm). This in order to homogenise the

* Corresponding author. Tel.: +52 (55) 5622 4640; fax: +52 (55) 5616 1371.
E-mail address: lima@iim.unam.mx (E. Lima).

1387-1811/$ - see front matter © 2011 Elsevier Inc. All rights reserved.
doi:10.1016/j.micromeso.2011.06.031

cation exchange capacity of natural zeolite, it was converted to a homoionic sodium form as follows: zeolite material was treated with a 5 M NaCl solution for 8 days and washed with deionised water until no chloride ions were detected. The Na-treated, clinoptilolite-rich tuff was then dried at 80 K for 12 h. After this treatment the formula of zeolite was as follows: $Na_{1.8}K_{0.1}Ca_{0.05}(Al_2Si_{10}O_{24})\cdot 17H_2O$. Variations in the composition of clinoptilolite from Oaxaca have been reported previously [21].

2.2. Silver containing zeolites

Sodium clinoptilolite zeolite (5 g) was shaken for 3 h in 100 mL of a 0.1 M (or 0.05) solution of $AgNO_3$. The samples were then separated by centrifugation and dried at 80 °C. Later, samples were reduced at 550 (or 700) °C under H_2 (5 mL/min) for 4 h. Table 1 summarises the samples being studied. The nomenclature adopted was ClinoAg-X-Y, where X is the reduced temperature, and Y is the amount of silver (wt%) as determined by X-ray fluorescence (a calibration curve was previously drawn).

2.3. Characterisation

X-ray diffraction patterns of the samples were obtained on a Siemens D500 diffractometer with a copper X-ray anode tube. K radiation (wavelength of 1.315 Å) was selected with a diffracted beam monochromator. Small-angle X-ray scattering (SAXS) curves were acquired using a Kratky camera coupled to a copper anode tube. The SAXS data were processed with the ITP program [22–26], where the angular parameter (h) is defined as $h = 4\pi \sin\theta/\lambda$, where θ and λ are the X-ray scattering angle and wavelength, respectively. The obtained data can be described by $I(q) = \sum_i I_i(0)\exp[(-R_{gi}q)^2/3]$, where $I_i(0)$ denotes the scattering intensity at $q = 0$ of the scattering centre i with the radius of gyration R_{gi} [27]. The shape of the scattering objects was estimated from the Kratky plot, i.e., $h^2I(h)$ against h. The shape is determined depending on the Kratky curve profile. For instance, the scattering curve for the globular conformation follows the Porod law, where $I(h)$ is proportional to h^{-4} for large h values and to h^{-2} for moderate h values. Hence, the Kratky plot exhibits a clear peak in the case of spherical particles. If a shape can be assumed, the size distribution function may be calculated. Lastly, from the slope of the curve log $I(h)$ vs log(h), the fractal dimension of the scattering objects was evaluated. It is worth notice that by the Babinet principle, the small-angle X-ray scattering may be due either to dense particles in a low-density environment or to pores or low-density inclusions in a continuous high electron density medium. Then, in order to characterise only the silver phase, we have subtracted the SAXS data of the free-silver zeolite from those of the silver-loaded zeolite. This method was earlier shown to be efficient in the characterisation of particles supported onto porous materials [28–30].

Solid-state ^{27}Al and ^{29}Si Nuclear Magnetic Resonance (NMR) single excitation experiments were performed on a Bruker Avance 400 spectrometer at frequencies of 104.2 and 79.4 MHz, respectively. ^{29}Si NMR spectra were acquired using the combined techniques of Magic Angle Spinning (MAS) and Proton Dipolar Decoupling (HPDEC). Direct pulsed NMR excitation was used throughout, employing 90° observing pulses (3 μs) with a pulse repetition time of 40 s. Powdered samples were packed in zirconia rotors. The spinning rate was 5 kHz. Chemical shifts were referenced to TMS. ^{27}Al MAS NMR spectra were acquired using short single pulses ($\pi/12$) and a delay of 0.5 s. The samples were spun at 10 kHz, and the chemical shifts were referenced to an aqueous 1 M $AlCl_3$ solution.

Table 1
Content of Ag-clinoptilolite samples prepared under different conditions.

Code sample	Solution used during Na–Ag exchange	Temperature of reduction (°C)	Silver content[a] (wt%)
ClinoAg-500-2.1	$AgNO_3$ 0.05 M	500	2.1
ClinoAg-700-2.1	Ag NO_3 0.05 M	700	2.1
ClinoAg-500-4.0	Ag NO_3 0.10 M	500	4.0
ClinoAg-700-4.0	Ag NO_3 0.10 M	700	4.0

[a] As determined by X-ray fluorescence.

2.4. Bacteria experiments

E. coli and *Salmonella typhi* were acquired from ENCB Mexico. Tripticaseine broth medium was used for growing and maintaining the bacterial cultures. For the growth experiments, a starter culture of each strain was inoculated with fresh colonies and incubated for 24 h in Tripticaseine medium. Bacterial growth rates were determined by counting the number of surviving colonies in a selective agar. Fresh medium (18 mL) was inoculated in test tubes with the starter culture and grown at 35.5 °C with continuous agitation at 30 rpm. Variable amounts of Ag zeolite were then added to the culture, and the colonies were measured over a time course. During all experiments treated with bacteria the material used was sterilized and zeolite used immediately after preparation.

3. Results and discussion

3.1. Structural and textural properties of Ag-clinoptilolite

Fig. 1 displays the XRD patterns of four samples under study. All materials exhibited peaks due to clinoptilolite zeolite. In addition, the samples with the highest amount of silver presented well-defined narrow peaks attributable to metallic silver, labelled in the figure with Ag. A higher amount of silver produced more intense Ag XRD peaks. No significant differences were observed within XRD technique limits or between samples with the same content of silver reduced at different temperatures. These results clearly indicate that the zeolite structure was preserved after silver deposition. At low concentrations, the metallic silver was well dispersed in both internal (microporous) and external surfaces. An increase in silver resulted in small particles agglomerating to form larger particles; these particles were mainly located at the external surface of the zeolite.

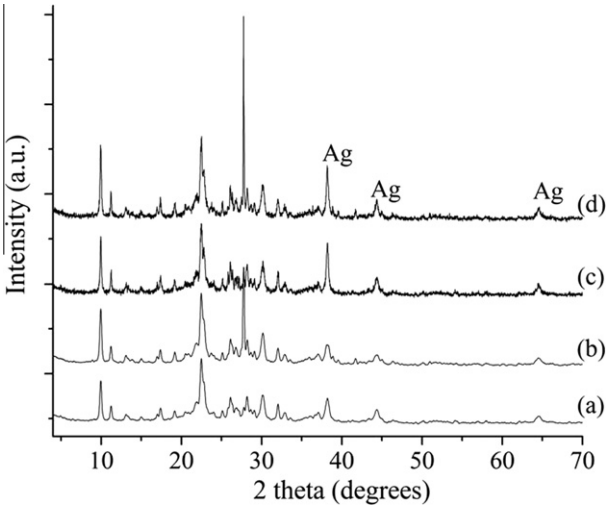

Fig. 1. X-ray diffraction patterns of Ag-clinoptilolite samples before test as biocide of *E. coli* and *Salmonella typhi*. ClinoAg-500-2.1 (a); ClinoAg-700-2.1 (b); ClinoAg-500-4.0 (c) and ClinoAg-700-4.0 (d).

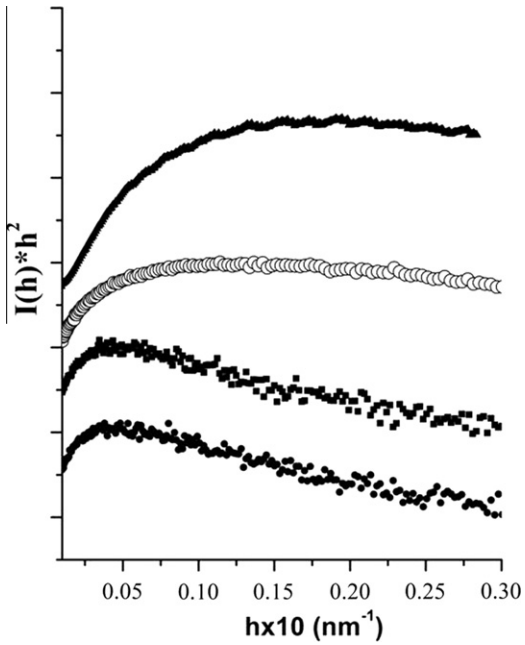

Fig. 2. Kratky profiles of ClinoAg-500-2.1 (–■–), ClinoAg-700-2.1 (–▲–), ClinoAg-500-4.0 (–●–) and ClinoAg-700-4.0 (–○–).

Fig. 2 shows a comparison of the Kratky plots of four Ag-clinoptilolite samples; all samples presented the typical profile of globular heterogeneities [31]. As the metal particles were scattered, it is evident that spherical silver particles were deposited on the zeolite support. The size distributions of the particles were calculated assuming spherical shapes (Fig. 3). The two samples with the lowest amount of silver appeared to have size distributions that ranged from 0.7 to 8 nm (radius). When a sample was reduced at 500 °C, a multimodal distribution with maxima at 1.1, 3.2 and 6.6 nm was obtained. Most of the particles studied were in the range of 4.5–8 nm. Conversely, if the reduction temperature was increased to 700 °C, maxima at 0.9, 3.1, 5.2 and 7.4 nm were observed, with the majority of the particle sizes measuring between 1.8 and 6.4 nm. The size distribution was modified with an increase in silver content. Particles with radii as small as 0.7 nm were detected, but the peaks were broader than in samples reduced at 500 °C. In fact, in sample ClinoAg-700-4, two very broad peaks centred at 5.5 and 9.2 nm were observed, demonstrating that high temperature and high loading leads to a more heterogeneous distribution of silver and induces the sintering of smaller particles.

Fractal dimension values of the scattered objects in the Ag-zeolite samples were calculated from the SAXS data under the Porod law [32,33]; they are reported in Table 2. It is evident that a higher temperature of reduction results in higher fractal dimension, suggesting that larger and denser particles are created. Due to the size of these particles, it is assumed that they are located at the external surface of the material, i.e., outside of the zeolite channels.

Fig. 4 shows a comparison between the ^{29}Si MAS NMR spectra of the samples. Four resonance lines at −95, −101, −108 and −113 ppm were identified after deconvolution, which correspond to Si(2Al), Si(1Al), Si(1Al) and Si(0Al) configurations, respectively [34]. All four samples present similar spectra, suggesting that the siliceous framework is not modified by the incorporation of silver and thermal treatments.

The ^{27}Al MAS NMR spectra, Fig. 5, show that aluminium remained tetrahedrally coordinated (signal at 56 ppm) [35], independently of the amount of silver or the temperature of reduction. It was noted, however, that in the spectra of materials with the

Table 2
Fractal dimension values of Ag-clinoptilolite samples, as determined by SAXS data.

Code sample	Fractal dimension
ClinoAg-500-2.1	2.33
ClinoAg-700-2.1	2.69
ClinoAg-500-4.0	2.35
ClinoAg-700-4.0	2.91

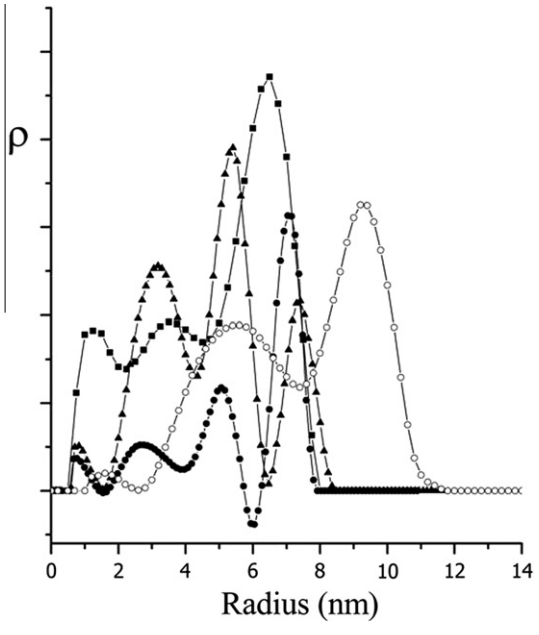

Fig. 3. Size distribution of silver particles as determined by SAXS for ClinoAg-500-2.1 (–■–), ClinoAg-700-2.1 (–▲–), ClinoAg-500-4.0 (–●–) and ClinoAg-700-4.0 (–○–).

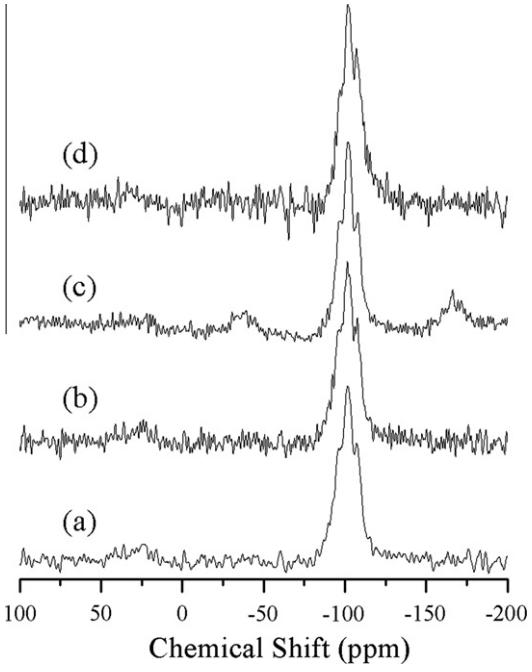

Fig. 4. ^{29}Si MAS NMR spectra of silver-containing clinoptilolite samples. ClinoAg-500-2.1 (a); ClinoAg-700-2.1 (b); ClinoAg-500-4.0 (c) and ClinoAg-700-4.0 (d).

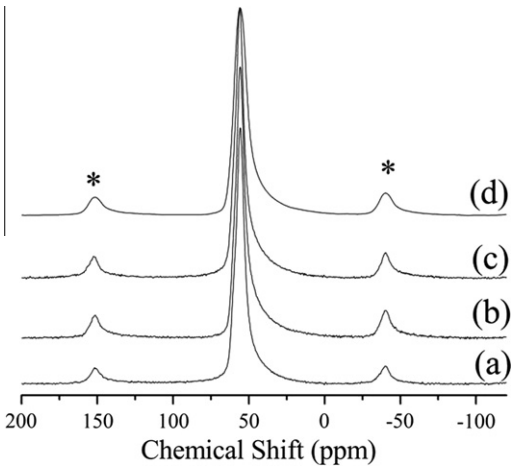

Fig. 5. ^{27}Al MAS NMR spectra of silver-containing clinoptilolite samples. ClinoAg-500-2.1 (a); ClinoAg-700-2.1 (b); ClinoAg-500-4.0 (c) and ClinoAg-700-4.0 (d).

highest load of silver, the resonance peak became slowly broader that in other samples. This is because the quadrupole of aluminium nuclei senses a higher electronic density coming from the silver particles. This result suggests that at high loads of silver, some Ag particles are incorporated into the micropores, and others agglomerate onto the free spaces of the zeolite particles.

3.2. Ag-clinoptilolite as a biocide for E. coli

Fig. 6 shows that the colonies survived as time went on in the culture media in the presence of different Ag-clinoptilolite samples. The amount of ClinoAg-X-Y sample was 0.06 g per 18 mL of culture media. As a reference sample, the zeolite free of silver was also tested. In this case, the number of colonies increased rapidly with time. In the case of silver-containing zeolites, it was clear that the amount of silver had an effect on the biocidal properties of the material. With a load of 4 wt% of silver, independently of the reduction temperature, the zeolite eliminated all colonies in times as short as 30 min. On the contrary, the samples with the lowest amount of silver allowed the development of microorganisms during the first 30 min. A decrease in the number of colonies was observed after 60 min, but all bacteria were killed only after 120 min. Thus, it seems that the distribution of silver on the surface of the material is a crucial parameter to obtain efficient biocidal materials. At high Ag loads, bacteria have rapid contact with large, dense silver particles dispersed at the external surface of the zeolite. At low Ag loads, bacteria are initially dispersed on the zeolite enhancing their development. With time, however, the bacteria have contact with silver sites located in the channels of the zeolite and other sites at the external surface.

Note that the relationship between the mass of Ag zeolite and the volume of the culture media that we have used in the case of the zeolite loaded with 4 wt% of silver appears to be very efficient as bacteria survived only for a very short period of time. Thus, we have carried out another series of experiments in which the amount of ClinoAg-X-Y sample was 0.03 g per 18 mL of broth. Fig. 7 compares the curves of the number of colonies as a function of time when 0.03 g as well as 0.06 g of biocidal zeolite sample was used. A lower amount of Clino-Ag resulted in a longer time needed to reach the minimum number of survived colonies. When ClinoAg-700-2.1 was used, an increase in the number of colonies was observed for times as short as 20–30 min. This was followed by a

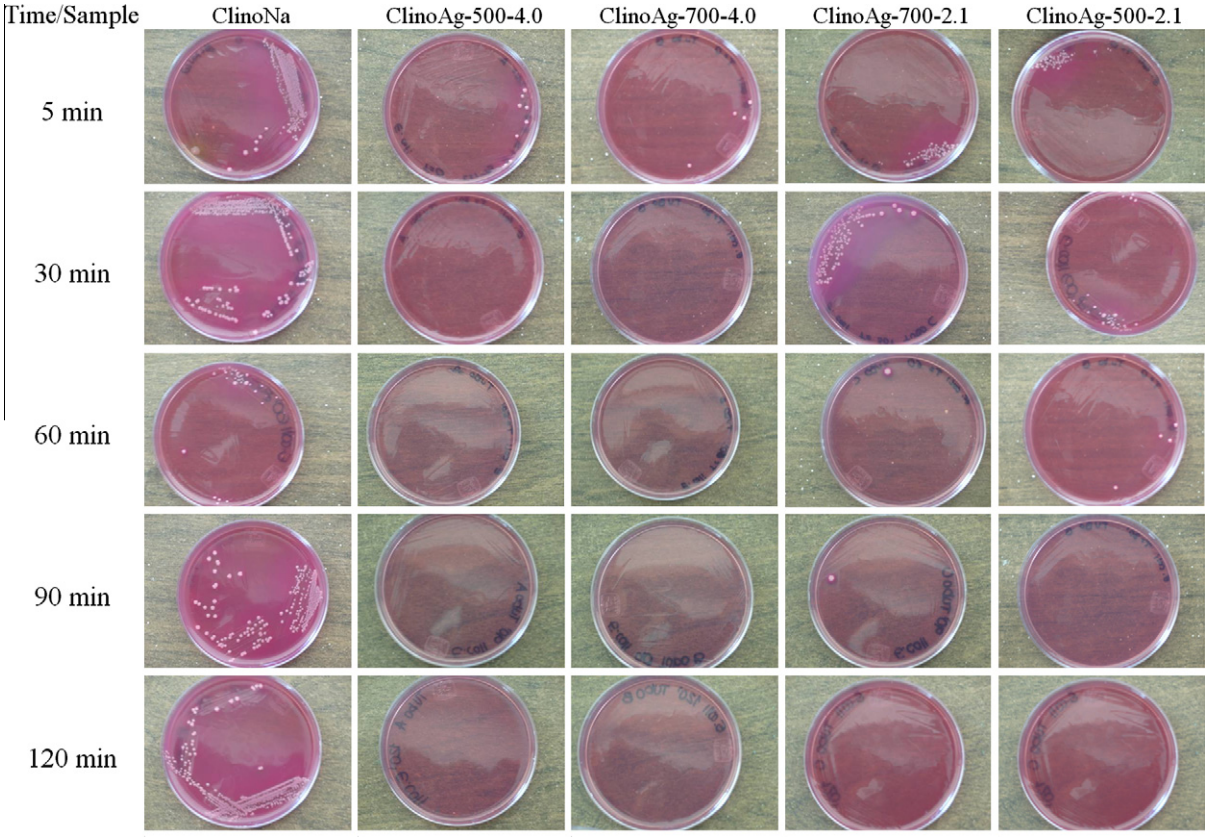

Fig. 6. Colonies of *E. coli* surviving after culture media was exposed to 0.06 g of ClinoAg-X-Y.

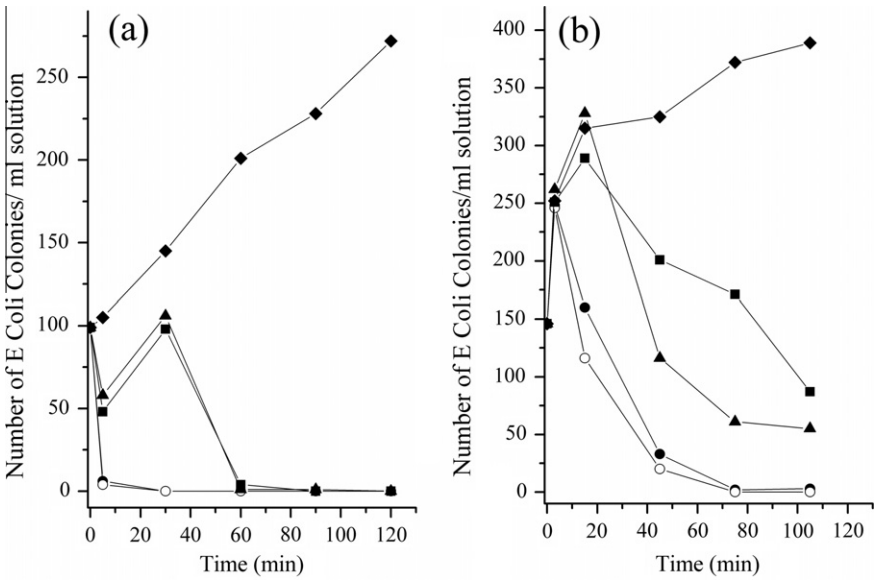

Fig. 7. Evolution as a function of time of number of *E. coli* colonies survived in culture media in the presence of ClinoNa (–♦–), ClinoAg-500-2.1 (–■–), ClinoAg-700-2.1 (–▲–), ClinoAg-500-4.0 (–●–) and ClinoAg-700-4.0 (–○–). Amount of zeolite was 0.06 g (a) or 0.03 g (b).

clear decrease until the total extinction of bacteria was reached with 0.06 g. As shown by SAXS, this sample exhibited a high amount of spheroid particles with diameters between 3 and 6 nm. It seems then that these particles are not immediately accessible to bacteria, possibly because the particles are stabilised upon entering the channels. When these particles are not accessible, bacteria use the external surface to increase the number of colonies. However, when the majority of the silver particles become accessible, the bacteria are rapidly killed.

3.3. Ag-clinoptilolite as a biocide for S. typhi

Fig. 8 shows that the bacteria colonies survived in the presence of the Clino-Ag materials. The behaviour observed in the development of *Salmonella* differed from that observed in *E. coli.* At short times, *Salmonella* growth was preferably inhibited by medium-size particles with a moderate bulk density (fractal dimension far from 3) stabilised on sample ClinoAg-700-2.1. However, this sample contained a high number of colonies. The

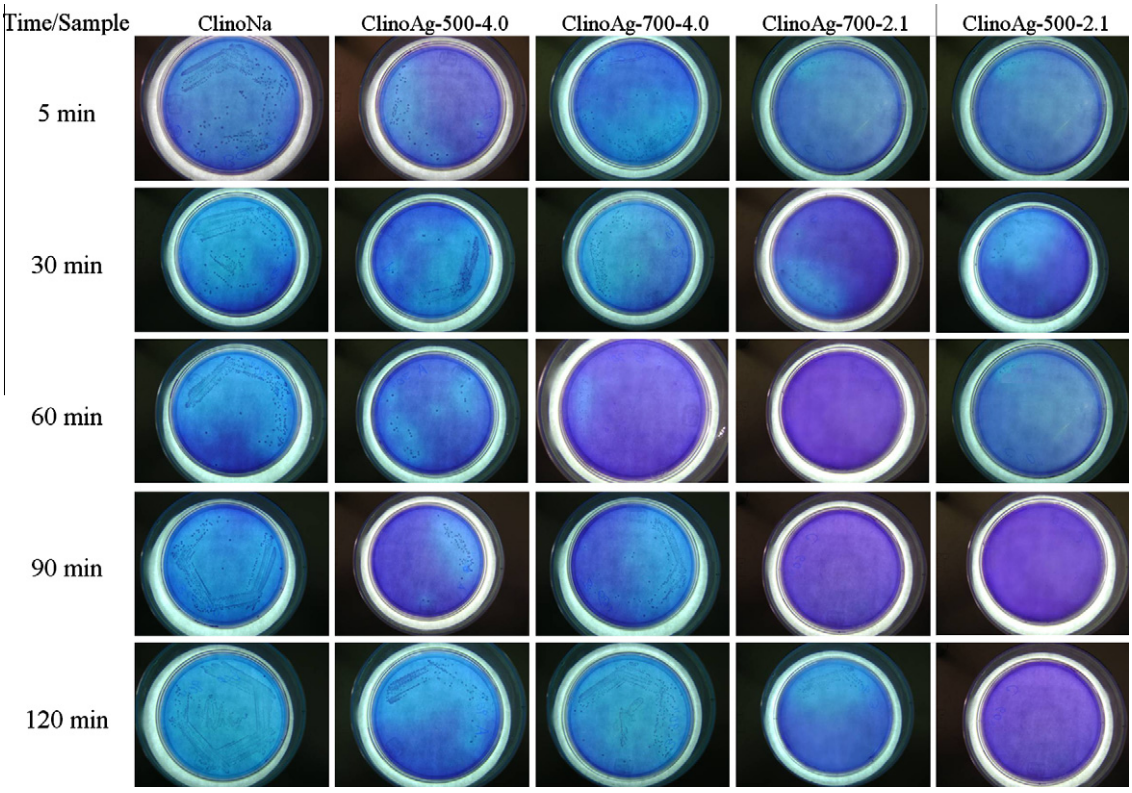

Fig. 8. Colonies of *Salmonella typhi* surviving after culture media was exposed to 0.06 g of ClinoAg-X-Y.

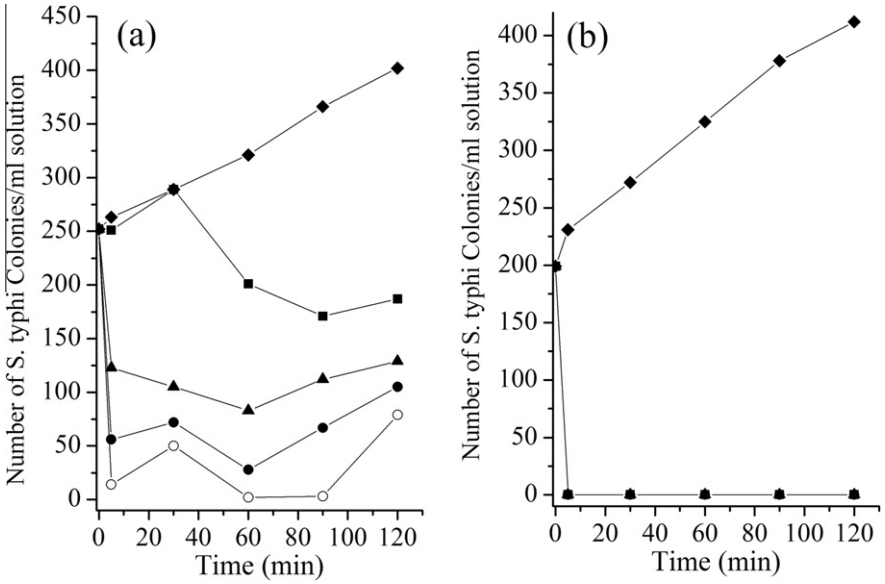

Fig. 9. Evolution as time went on of number of *Salmonella typhi* colonies survived in culture media in the presence of ClinoNa (–♦–), ClinoAg-500-2.1 (–■–), ClinoAg-700-2.1 ClinoAg-500-4.0 (–●–) and ClinoAg-700-4.0 (–○–). Amount of zeolite was 0.06 g (a) or 0.12 g (b).

highest percentage of killed bacteria with this material was 30% in 65 min (Fig. 9). At longer times, the material was no longer effective, and an increase in the number of colony numbers was observed. In the presence of samples with a high loading of silver, the *Salmonella* colonies increased at short times independently of the reduction temperature. This was followed by a decrease and a subsequent increase for times longer than 90 min. Apparently, these samples were less efficient than sample ClinoAg-700-2.1. It should be noted, however, that the number of colonies in samples with high silver loading was never as high as that in sample ClinoAg-700-2.1. Thus, this result suggests that the amount of silver plays a crucial role in the biocide properties of Clino-Ag materials, and 0.06 g of this material is insufficient to completely eliminate the colonies of *Salmonella*. Therefore, the experiments were repeated with a high amount of biocide material. Fig. 9 compares the results obtained with 0.06 and 0.012 g of zeolite. At high amounts of Ag-zeolite, all the samples tested were able to completely eliminate the *Salmonella* colonies at very short times. It can be concluded that at very high concentrations of silver, the shape and size of the silver particles dispersed on the surface of the support are not crucial.

3.4. Ag-clinoptilolite after biocide tests

In order to verify the potential reuse of biocidal materials. At end of experiments with bacteria, solutions were analysed and not silver was detected within limits of atomic absorption spectroscopy. Further, the Ag-clinoptilolite zeolites were recuperated, washed and reduced under hydrogen after booth biocide tests were conducted with *Salmonella* and *E. coli.* No significant differences were observed in the characterisation of these samples and those that were synthesised. For the sake of conciseness, the spectra and X-ray diffraction patterns of the samples studied after biocide tests were not included in this manuscript.

4. Conclusion

Metallic silver nanoparticles supported on clinoptilolite zeolite are excellent biocides to eliminate *E. coli* present in water at times as short as 60 min. The performance of the material is determined by the amount of silver supported on the zeolite, the distribution on the surface (micropores and outer surface), the size of the particles and the fractal dimension of the metallic particles. In the case of *S. typhi*, however, the silver nanoparticles supported are less efficient as biocides than in the case of *E. coli.* In order to completely eliminate *Salmonella* colonies, a high amount of silver-zeolite was required. Silver did not leach from the zeolite during the experiments with both *E. coli* and *Salmonella*; thus, we can conclude that the biocidal materials can be reused.

References

[1] J. Dou, X. Liu, A. Ding, J. Hazard. Mater. 165 (2009) 325–331.
[2] A. Gangagni Rao, P. Ravichandra, Johny Joseph, Annapurna Jetty, P.N. Sarma, J. Hazard. Mater. 147 (2007) 718–725.
[3] I. Chopra, J. Antimicrob. Chemother. 59 (2007) 587–590.
[4] A. Łukasiewicz, D. K Chmielewska, L. Waliś, L. Rowińska, Pol. J. Chem. Technol. 5 (2003) 20–22.
[5] Y. Wan, D. Zhang, Y. Wang, P. Qi, J. Wu, B. Hou, J. Hazard. Mater. 186 (2011) 306–312.
[6] S.H. Jeong, Y.H. Hwang, S.C. Yi, J. Mater. Sci. 40 (2005) 5413–5418.
[7] N. George, J. Faoagali, M. Muller, Burns 23 (1997) 493–495.
[8] S. Silver, L.T. Phung, J. Indust. Microbiol. Biotechnol. 33 (2006) 627–634.
[9] C.G. Gemmell, D.I. Edwards, A.P. Fraise, J. Antimicrob. Chemother. 57 (2006) 589–608.
[10] R.H. Demling, L. De Santi, Wounds 13 (2001) 5–14.
[11] O. Eksik, T. Erciyes, Y. Yagci, J. Macromol. Sci. Part A. Pure Appl Chem. 45 (2008) 698–704.
[12] H.J. Lee, S.Y. Yeo, S.H. Jeong, J. Mater. Sci. 38 (2003) 2199–2204.
[13] E. Aneggi, J. Llorca, C. de Leitenburg, G. Dolcettia, A. Trovarelli, Appl. Catal. B-Environ. 91 (2009) 489–498.
[14] A. Montesinos-Castellanos, E. Lima, J.A. de los Reyes, H.V. Lara, J. Phys. Chem. C 111 (2007) 13898–13904.
[15] S. Sabbani, D. Gallego-Perez, A. Nagy, W.J. Waldman, D. Hansford, P.K. Dutta, Micropor. Mesopor. Mater. 135 (2010) 131–136.
[16] K. Shameli, M.B. Ahmad, M. Zargar, W.M.Z.W. Yunus, N.A. Ibrahim, Int. J. Nanomed. 6 (2011) 331–341.
[17] K. Shameli, M.B. Ahmad, M. Zargar, W.M.Z.W. Yunus, N.A. Ibrahim, M.G. Moghaddam, Int. J. Nanomed. 6 (2011) 271–284.
[18] M.M. Llanes-Monter, M.T. Olguín, Env. Sci. Pol. Res. 14 (2007) 397–403.
[19] K. Pavelić, M. Hadžija, L. Bedrica, J. Pavelić, I. Đikić, M. Katić, M. Kralj, M. Bosnar, S. Kapitanović, M. Poljak-Blaži, J. Mol. Med. 78 (2001) 708–720.
[20] J. Hrenovic, M. Rozic, L. Sekovanic, A. Anic-Vucinic, J. Hazard. Mater. 156 (2008) 576–582.
[21] N.A. Hernández-Beltrán, M.T. Olguín, Hydrometallurgy 89 (2007) 374–378.
[22] O. Glatter, J. Appl. Crystallogr. 14 (1981) 101–108.
[23] O. Glatter, B. Hainisch, J. Appl. Crystallogr. 17 (1984) 435–441.
[24] O. Glatter, J. Appl. Crystallogr. 21 (1988) 886–890.

[25] O. Glatter, Prog. Colloid. Polym. Sci. 84 (1991) 46–54.
[26] O. Glatter, K. Gruber, J. Appl. Crystallogr. 26 (1993) 512–518.
[27] A. Guinier, G. Foumet, Small-Angle Scattering of X-rays, Wiley, New York, 1955, p. 25.
[28] V. Schiinemann, H. Winkler, Ch. Butzlaff, A.X. Trautwein, Hyperfine Interact. 93 (1994) 1427–1432.
[29] L. Pajak, B. Bierska-Piech, J. Mrowiec-Bialon, A.B. Jarzebski, R. Diduszko, Fibres and Textiles 13 (2005) 69–74.
[30] E. Lima, A. Guzmán-Vargas, J. Méndez-Vivar, H. Pfeiffer, J. Fraissard, Catal. Lett. 120 (2008) 244–251.
[31] M. Kataoka, J.M. Flanagan, F. Tokunaga, D.M. Engelman, Use of X-ray solution scattering for protein folding study, in: B. Chanse, J. Deisenhofer, S. Ebashi, D.T. Goodhead, H.E. Huxley (Eds.), Synchrotron Radiation in the Biosciences, vol 4, Clarendon Press, Oxford, UK, 1994, p. 87.
[32] A. Harrison, Fractals in Chemistry, Oxford University Press, New York, 1995.
[33] J.E. Martin, A.J. Hurd, J. Appl. Crystallogr. 20 (1987) 61–78.
[34] C.A. Fyfe, G.C. Gobbi, W.J. Murphy, R.S. Ozubko, D.A. Slack, J. Am. Chem. Soc. 106 (1984) 4435–4438.
[35] E. Lippmaa, M. Magi, A. Samoson, G. Engelhardt, A.R. Grimmer, J. Am. Chem. Soc. 102 (1980) 4889–4893.